
**Liquid Crystals**
Publication details, including instructions for authors and subscription information:
http://www.informaworld.com/smpp/title~content=t713926090

# Synthesis, Characterization and X-Ray Diffraction Studies of a New Homologous Series of Cyano-Substituted Mesomorphic Side Chain Polyacrylates

P. Davidson[a]; L. Strzelecki[a]
[a] Laboratoire de Physique des Solides, Universite Paris-Sud associe au CNRS, Orsay Cedex, France

**To cite this Article** Davidson, P. and Strzelecki, L.(1988) 'Synthesis, Characterization and X-Ray Diffraction Studies of a New Homologous Series of Cyano-Substituted Mesomorphic Side Chain Polyacrylates', Liquid Crystals, 3: 11, 1583 — 1595
**To link to this Article: DOI:** 10.1080/02678298808086697
**URL:** http://dx.doi.org/10.1080/02678298808086697

LIQUID CRYSTALS, 1988, VOL. 3, NO. 11, 1583–1595

# Synthesis, characterization and X-ray diffraction studies of a new homologous series of cyano-substituted mesomorphic side chain polyacrylates

by P. DAVIDSON and L. STRZELECKI

Laboratoire de Physique des Solides, associé au CNRS, Bâtiment 510, Université Paris-Sud, 91405 Orsay Cédex, France

*(Received 23 May 1988; accepted 18 June 1988)*

A new series of cyano-substituted mesomorphic side chain polyacrylates has been synthesized. Optical observations, D.S.C. studies and X-ray diffraction on oriented samples show that all polymers possess a partially bilayer $S_{A_d}$ phase. The smectic period has been measured from which it is inferred that the molecular structure of the mesogenic cores (i.e. the presence of $\pi$-systems and antiparallel dipoles) induces a small overlap ($d \approx 1{\cdot}71$). The X-ray patterns show that for the whole series, the third order reflection is the most intense. By inverse Fourier transform, we derive the projection of the electron density profile along the director which we try to explain in terms of the molecular features.



## 1. Introduction

Since the original works of Ringsdorf, Finkelmann and co-workers [1, 2], the development of mesomorphic side chain polymers has been considerable. By applying the flexible spacer concept [1], several homologous series of cyano-substituted mesomorphic side chain polymers have been synthesized [3]. It is well-known from the study of polar low molecular weight mesogens that the presence of a terminal-CN group induces a strong longitudinal dipole in the mesogenic core. These compounds often possess smectic A phases of the $S_{A_d}$ type [4]. In such phases, the dipoles result in pairs of antiparallel molecules. The length of these pairs depends on the molecular structure of the mesogenic core. The presence of the $\pi$-systems and of other dipoles pointing in the same direction as that of the -CN group favours a delocalization of the dipole along the core. Then, the length of a molecular pair, $d$, is close to the length of the molecule, $l$, ($d < 1{\cdot}5l$). Conversely, if the other dipoles point in the direction opposite to that of the -CN group, then the CN dipole remains localized and there is a small overlap ($d \approx 2l$). This is the case of the alkylphenylcyanobenzoyloxybenzoate (DBn) series which shows a rich polymorphism [4, 5]. (Actually, the overlap also depends on the length of the aliphatic tail.)

For most of the cyano-substituted side chain polymers found in the literature, the chemical structure is such that the overlap is important. We have synthesized a new homologous series in which the chemical structure of the rigid cores looks like that of the DBn series, except that they possess only two instead of three phenyl rings. Though we do not find a rich polymorphism, these polymers still possess some interesting structural properties.

## 2. Synthesis and characterization

We have synthesized a homologous series of eight polymers labelled: poly[4(4′-cyanobenzoyloxy)benzoyloxy $\omega$-*n*-alkylacrylate]s **1**, of formula:

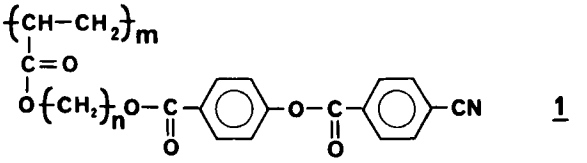

**1**

they are denoted by: $P_n$. Note that the two $-O_2C-$ dipoles are set in a direction antiparallel to that of the -CN group, and so the CN dipole should remain localized.

The synthesis has been performed according to the scheme:

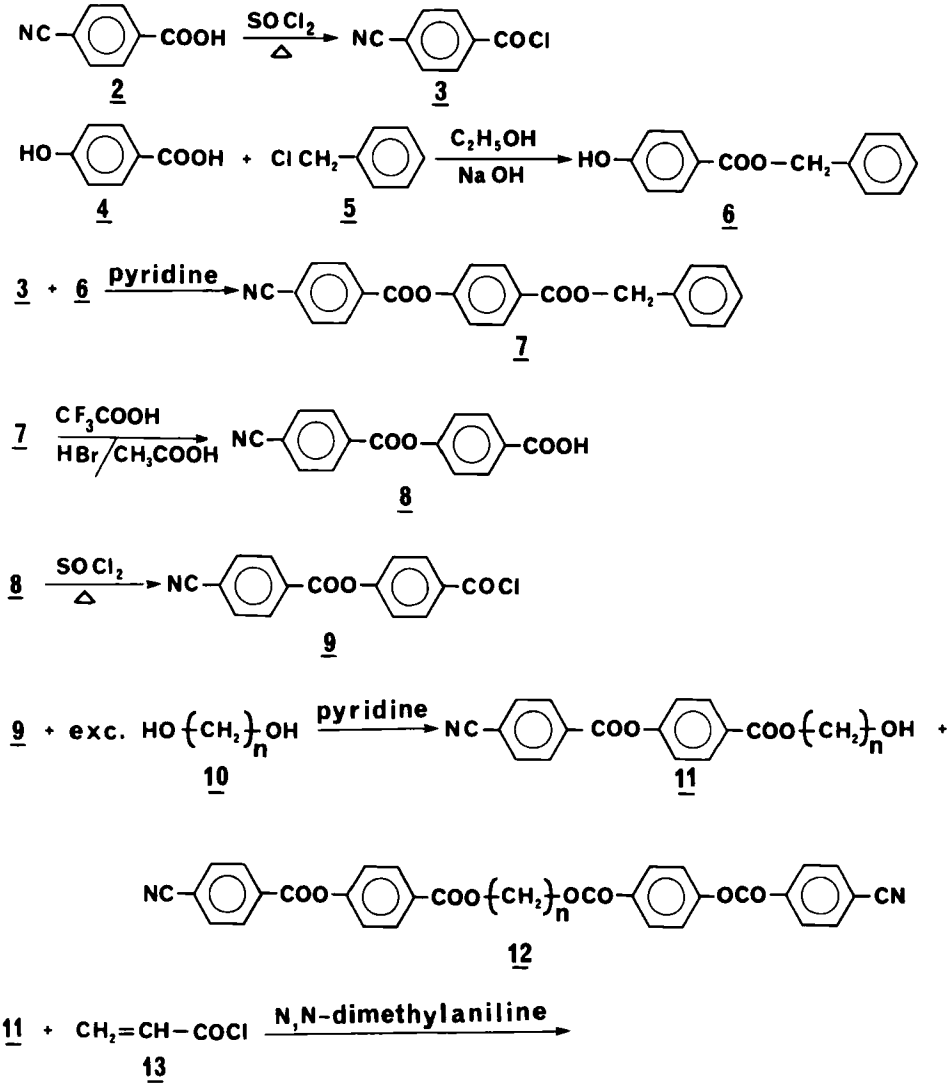

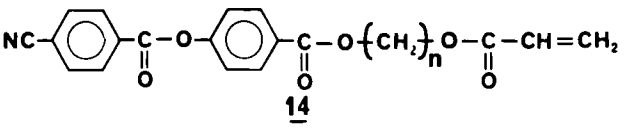

**14**

The experimental procedure is described in the Appendix.

The polymorphism has been identified and the transition temperatures have been first measured using a polarizing microscope (Leitz orthoplan-pol) equipped with a heating stage (Mettler FP5) and confirmed by differential scanning calorimetry (Mettler DSC 30). The results are summarized in table 1. All polymers show only a smectic A phase except $P_{12}$ which exhibits a more complicated polymorphism. Figure 1 (*a*) represents a typical D.S.C. curve of the series $P_4$–$P_{10}$; $T_g$ and $T_{S_AI}$ can be seen clearly. The D.S.C. curve for $P_{12}$ reveals the existence of several phases (see figure 1 (*b*)).

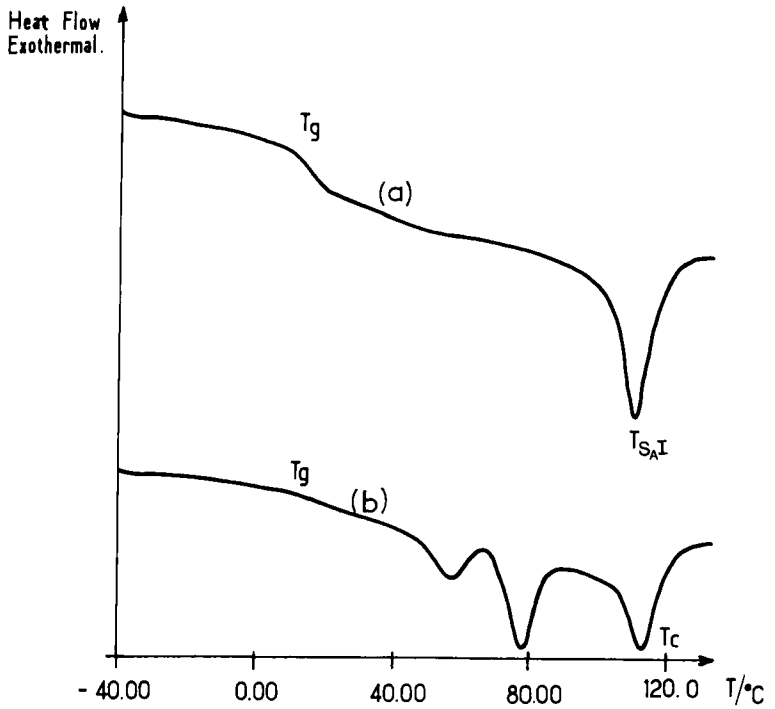


Figure 1. D.S.C. curves for polymers $P_8$ and $P_{12}$. Heating rate 20 K/min; $T_g$, glass transition; $T_{S_AI}$, smectic A–isotropic transition. (*a*) Polymer $P_8$ typical of the series $n$ = 4–10. (*b*) Polymer $P_{12}$ presents two crystalline phases below the smectic A phase.

The inherent viscosity measurements have been performed in chloroform (0·5 g.dl$^{-1}$) at a temperature of 25°C using a microviscometer (KPG-Ubbelhode Schott Gerate GmbH) equipped with a capillary tube No 1. These measurements show that the degree of polymerization for the various $P_n$ are comparable. $T_g$ is seen to decrease as the spacer length increases; this is the usual internal plasticizing effect.

Table 1. Transition temperatures and inherent viscosities of the polymers $P_n$. $T_g$, glass transition; $T_{S_AI}$, smectic A–isotropic transition; $K_1$, $K_2$, crystalline phases.

| $n$ | $T_g$/°C | | | | | $T_{S_AI}$/°C | $\eta_{Inh}$ |
|---|---|---|---|---|---|---|---|
| 4 | 40 | | | | | 121 | 0·14 |
| 5 | 30 | | | | | 105 | 0·24 |
| 6 | 30 | | | | | 103 | 0·21 |
| 7 | 20 | | | | | 92 | 0·32 |
| 8 | 15 | | | | | 110 | 0·19 |
| 9 | 15 | | | | | 107 | 0·31 |
| 10 | 15 | | | | | 102 | 0·16 |
| 12 | 15 | $K_1$ | 60 | $K_2$ | 80 | 112 | 0·14 |

## 3. X-ray diffraction

### 3.1. *Experimental*

Only three polymers of the series have been studied thoroughly by X-ray diffraction: $P_5$, $P_8$, and $P_{12}$. Aligned samples could be obtained in two ways:

(*a*) by slowly cooling from the isotropic phase to the $S_A$ phase in a magnetic field of 1·7 T. This method proved efficient for polymers $P_8$ and $P_{12}$, but only a partial alignment appeared for polymer $P_5$. This polymer has the smallest spacer of the series and the coupling between the disordered backbone and the mesogenic cores may be too large to obtain good alignment (polymer $P_5$ may also have a slightly larger molecular weight and viscosity than polymers $P_8$ and $P_{12}$).

(*b*) by pulling fibres in the following way: the sample was held in a glass tube itself heated by a thermostatted oil bath. Fibres were produced by drawing a needle vertically that was initially immersed in the polymer melt above $T_{S_AI}$, by a system consisting of a counterweight and a pulley. Thus, the initial temperature of the sample as well as the drawing speed can be controlled. For all three polymers, oriented fibres could be produced.

According to a technique already described [6], the oriented samples were then examined in an evacuated camera using a point focussing X-ray beam [$\lambda$CuK$\alpha$ = 1·54 Å] obtained by reflection on doubly bent pyrolitic graphite.

### 3.2. *Results*

Figure 2 shows an X-ray diffraction pattern at room temperature of polymer $P_8$ aligned by a magnetic field. The pattern is typical of a $S_A$ phase:

along the meridian (direction of the magnetic field) and at small angles, three orders of reflection can be seen on the smectic layers. These Bragg spots (*a*) are resolution limited. (On the lower side, the first order reflection falls in the beam stop).

at wide angles and in a direction perpendicular to the meridian (equator), two diffuse crescents (*b*) are observed which show that the layers are liquid-like and that the mesogenic cores are oriented perpendicular to the layers; therefore, we have a $S_A$ phase as inferred from optical microscopy.

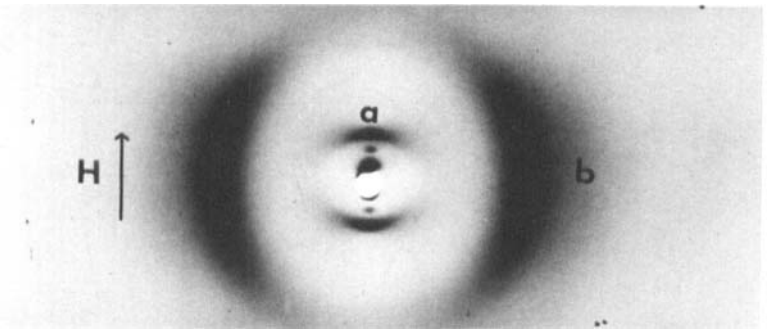


Figure 2. X-ray diffraction pattern of a magnetically aligned sample of polymer $P_8$ at room temperature. **H** is the direction of the magnetic field ($\lambda$CuK$\alpha$ = 1·54 Å); Sample-film distance: 60 mm.

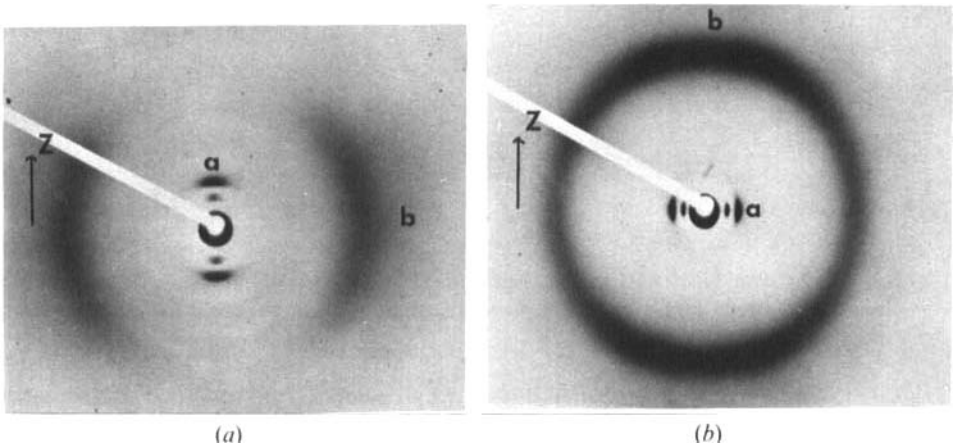


(*a*) (*b*)

Figure 3. X-ray diffraction patterns of oriented fibres of polymers $P_5$ and $P_{12}$. **Z** is the fibre axis ($\lambda$CuK$\alpha$ = 1·54 Å) at room temperature; sample film distance: 67 mm. (*a*) Polymer $P_5$. (*b*) Polymer $P_{12}$. (In each case, the first two Bragg spots fall in the beam stop.)

With increasing temperature, the pattern is preserved in the whole $S_A$ temperature range except for a slight blurring. Magnetically aligned samples of polymer $P_{12}$ between 80°C and 112°C show diffraction patterns similar to figure 2. Below 80°C, some sharp wide angle reflections are observed which indicate that both phases $K_1$ and $K_2$ are crystalline.

Figures 3(*a*) (*b*) show the X-ray diffraction patterns of fibres of polymers $P_5$ and $P_{12}$. The fibres are aligned and their patterns are similar to those of the magnetically aligned samples. However, a major difference exists between the fibres of polymer $P_8$ and $P_{12}$ on the one hand and that of polymer $P_5$ on the other: the polymer backbones are aligned along the stretching direction in the first case while the mesogenic cores are aligned along the stretching direction in the second. We do not know whether these different orientations result because of a difference in viscosity or in spacer length. (For polymer $P_{12}$, the smectic A structure is frozen at room temperature by the fast cooling).

The smectic periods, $d$, together with the lengths of the side chains, $l$, are shown in table 2 (the lengths $l$ are measured from Dreiding stereomodels in the most extended configuration and take into account the presence of the backbone). As expected, for each polymer the comparison between the values of $d$ and $l$ suggests that

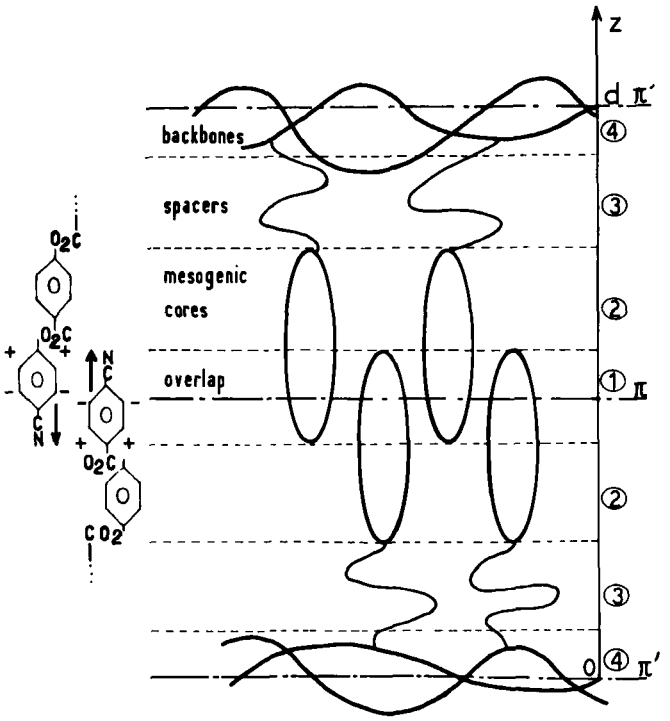


Figure 4. Schematic representation of the organization of the polymeric $S_{A_d}$ phase, $\pi$ and $\pi'$ are the planes of symmetry of the structure, regions (1) to (4) are to be compared with the corresponding sections of $\varrho(z)$.

Table 2. Smectic period, $d$, measured by X-ray diffraction. $l$, length of a side chain assuming a spacer in a fully extended conformation; $o$, overlap of the mesogenic cores ($o = 2l-d$).

| | $P_5$ | $P_8$ | $P_{12}$ |
|---|---|---|---|
| $d$ Å | 40 | 48 | 57 |
| $l$ Å | 24 | 28 | 33 |
| $o$ Å | 8 | 8 | 9 |

there is partial overlap of the mesogenic cores (see figure 4). Then, for all three polymers we can conclude that the smectic phase is of the $S_{A_d}$ type.

We now compare the smectic periods of this series with those already published. First, the overlaps shown in table 2 are rather small ($o \approx 8$ Å) compared with those published, for instance, by Mauzac *et al.* [3], ($o \approx 15$–$20$ Å) or by Sutherland *et al.* [7] ($o \approx 16$–$22$ Å). We can see here the influence of the molecular structure of the core. (For the polymers studied by Mauzac *et al.*, the presence of a single $O_2C$ dipole was not sufficient to ensure a small overlap). However, in our case we do not obtain $d \approx 2l$ but rather $d \approx 1{\cdot}7l$ and this may be due to the polymeric backbone which may increase the overlap in order to expand. We do not notice any influence of the spacer length on the overlap through it is seen in the series presented by Mauzac *et al.* and Sutherland *et al.* and also commonly in series of small molecules which possess three phenyl rings in their aromatic core.

### 3. Determination of the electron density profile along Oz

Oriented diffraction patterns (see figure 2) show that the most intense order of reflection is the third, and that for polymer $P_5$, the first order reflection is simply absent. This means that the ideal description [8] of a smectic A phase by a sinusoidal modulation of period $d$ along the director is not valid here. However, such a description is approximately correct for the smectic $A_d$ phase of low molecular weight polar mesogens [4] and therefore our distribution of intensities reflects the influence of the polymer backbones. We shall now try to derive some information about the organization of the $S_{A_d}$ phase from the intensities of the orders of reflection on the layers.

We call $\varrho(z)$ the projection of the electron density profile along the director. $\varrho(z)$ is a periodic function of period $d$ and can be expanded in a Fourier series. Since there is a partial overlap of the mesogenic cores, $\varrho(z)$ must be symmetrical with respect to planes perpendicular to the director [9]; these planes are sketched in figure 4. Then, the cosine terms are the only terms relevant in the Fourier series and we may write

$$\varrho(z) = \varrho_0 + 2 \sum_{n=1}^{\infty} A_n \cos\left(n2\pi \frac{z}{d}\right).$$

Since we do not measure $\varrho_0$, we have only access to the fluctuations of the density around its mean value and we shall keep:

$$\varrho(z) = \sum_{n=1}^{\infty} a_n \cos\left(n2\pi \frac{z}{d}\right).$$

By measuring the intensities of the Bragg reflections on powder patterns and correcting these values for the Lorentz factors, we obtain the moduli $|a_n|$. (The polarization corrections proved negligible at such low angles.) The values of the coefficients $|a_n|$ are listed in table 3.

Table 3. Intensities of the different orders of reflection on the smectic layers in powder diagrams and corresponding amplitudes corrected for the Lorentz factors, for polymers $P_5$, $P_8$ and $P_{12}$.

| | 1st order | 2nd order | 3rd order | |
|---|---|---|---|---|
| Measured intensity | 0 | 0·24 | 1 | Polymer $P_5$ room |
| Amplitude | $a_1 = 0$ | $a_2 = 0{\cdot}33$ | $a_3 = 1$ | temperature |
| Measured intensity | 1 | 0·04 | 0·40 | Polymer $P_8$ room |
| Amplitude | $a_1 = 0{\cdot}53$ | $a_2 = 0{\cdot}21$ | $a_3 = 1$ | temperature |
| Measured intensity | 1 | 0·11 | 0·15 | Polymer $P_{12}$ |
| Amplitude | $a_1 = 0{\cdot}85$ | $a_2 = 0{\cdot}56$ | $a_3 = 1$ | $T = 90°C$ |

The phase problem reduces to determining the signs of the $a_n$ coefficients: we must try every possible combination of signs and select the combinations which lead to physically acceptable $\varrho(z)$ functions.

In the following, we adopt the convention that, for instance, $\varrho_{+\,-\,+}(z)$ represents the combination where the coefficients $a_1$ and $a_3$ of the first and third orders of reflection are chosen positive and $a_2$ is taken to be negative. The case of polymer $P_5$ is simple because the first order reflection is absent, then we only have four

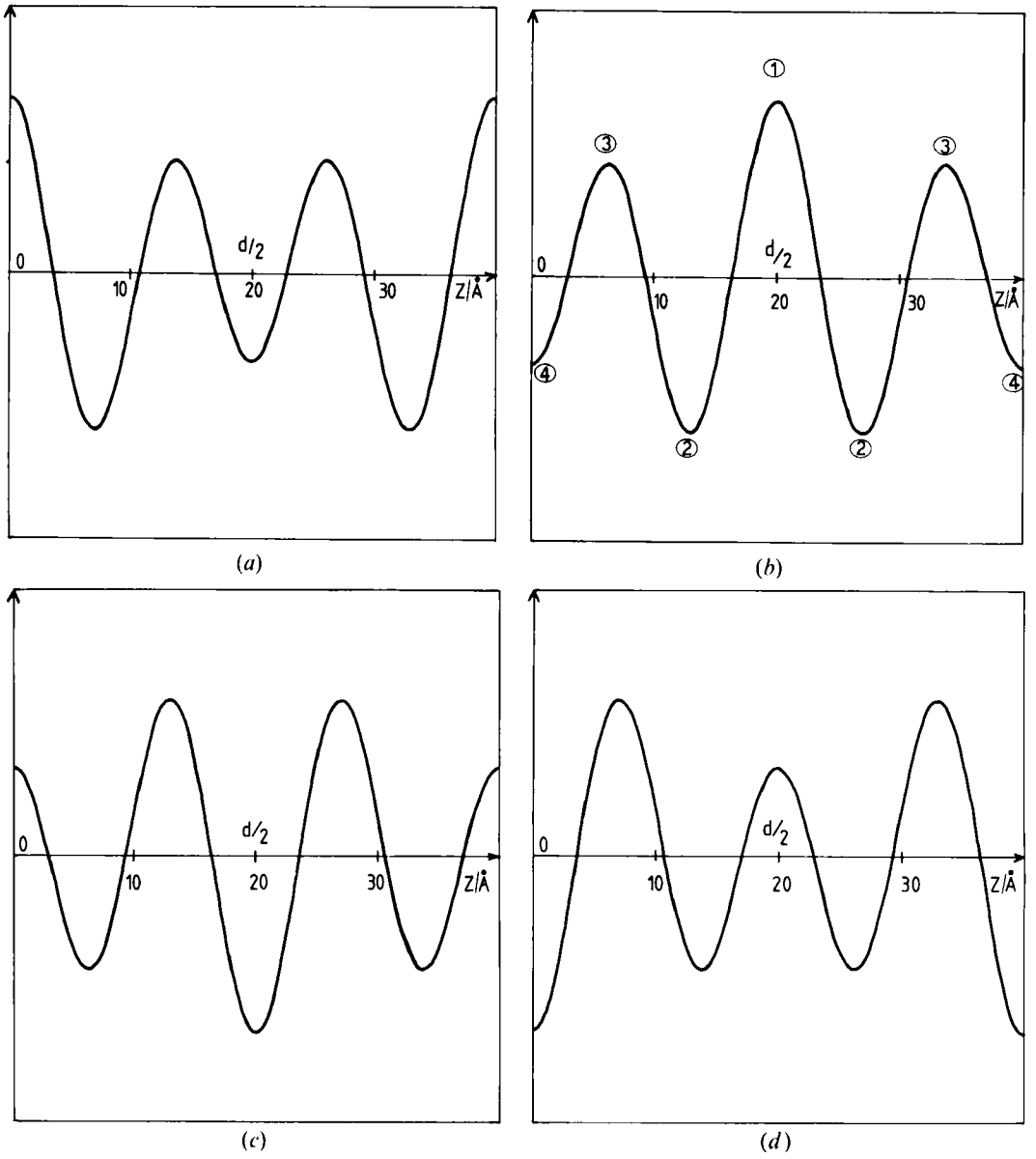


Figure 5. Different sign combinations of the second and third order harmonics to reproduce the projection of the electron density profile for polymer $P_5$; vertical scale in arbitrary units. The mean value of the electron density $\varrho_0$ is chosen equal to zero. (*a*) $\varrho_{0++}(z)$, (*b*) $\varrho_{0+-}(z)$, (*c*) $\varrho_{0-+}(z)$, (*d*) $\varrho_{0--}(z)$.

combinations possible: $\varrho_{0++}(z)$, $\varrho_{0+-}(z)$, $\varrho_{0-+}(z)$ and $\varrho_{0--}(z)$; they are represented in figure 5. (The scale of $\varrho(z)$ is chosen arbitrarily because we do not have any absolute measurements of the diffracted intensities.) We assume that the projection of the electron density profile along Oz reaches its highest value in the region of overlap of the mesogenic cores [9], then $\varrho(z)$ must present a single strong maximum and this rules out $\varrho_{0--+}(z)$ and $\varrho_{0---}(z)$. If we now notice that $\varrho_{0++}(z + d/2) = \varrho_{0+-}(z)$, then by assigning the origin of the Oz axis to the middle of the polymeric region, we recognize $\varrho_{0+-}(z)$ as the only physically acceptable solution.

At this point, we must try to interpret this projection of the electron density profile in terms of the molecular features. We have assigned the central maximum (1) of $\varrho_{0+-}(z)$ to the region of overlap (1) in figure 4. The packing of the mesogenic cores in this region determines their density within the smectic layer. This implies that in the regions (2) of mesogenic cores adjacent to the region of overlap the density must be smaller and this explains the minima (2) of $\varrho_{0+-}(z)$. Parts (3) and (4) of $\varrho_{0+-}(z)$ correspond to the aliphatic parts of the molecule and must be considered together. Part (3) is a secondary maximum which we attribute to the region of the spacers while part (4) is a secondary minimum which we attribute to the region of the polymeric backbones. These backbones resist the confinement between the layers by acting like springs on the flexible spacers. Thus the spacers will adopt disordered conformations and fill the free space induced in the organization by the partial bilayer packing of the cores. Therefore the projection of their electron density along $Oz$ should be increased compared to that of the polyacrylate backbones. Conversely, the backbones try to expand along the director and then the projection of their electron density should decrease. We know from the study of some polymeric $S_{A_1}$ phases ($d = l$) that when the polymer backbones are confined to two dimensions they give rise to some diffuse scattering [6]. The absence here of such diffuse scattering may indeed suggest that the polymeric backbones are not strictly confined. (This absence of diffuse scattering might also be due to the fact that our polyacrylates have a smaller molecular weight than that of the polymethacrylates described in [6]). Since this discussion is based on the intensities of the reflections on the smectic layers, we only deal with the mean values of the structural parameters: the overlap, the width of the backbone region etc. Hence figure 4 is only a schematic representation which does not include the important fluctuations that exist in such fluid systems.

The cases of polymers $P_8$ and $P_{12}$ are more complicated because the first order reflection is no longer absent. Then we have eight combinations possible and assuming again that $\varrho(z)$ must possess a central maximum, we are left with two possible solutions (see figure 6(*a*) to (*d*)). We would favour solution $\varrho_{-+-}(z)$ since the other solution gives the electron density of the spacers almost as high as that of the region of overlap. Anyway, the most important fact is that in all three cases and especially for polymer $P_5$, the electron density $\varrho(z)$ is dominated by the third harmonic. This may be explained by two reasons:

The overlap region has a mean size of about 8 Å and the mesogenic core has a size of approximately 15 Å, then region (2) has a mean size of 7 Å. Since the third harmonic must have six equidistant zeros, it may develop easily in a cell of size 40–50 Å. (Indeed we can see that the relative strength of the third harmonic is smaller for polymer $P_{12}$.) This explains why the cyano-substituted mesomorphic side chain polymers found in the literature which usually have larger overlaps do not display such a strong third order reflection.

To avoid the confinement between the layers, the backbones tend to expand and decrease the projection of their electron density. Conversely, the spacers are squeezed by the backbones and the projection of their electron density is increased. This oscillation of $\varrho(z)$ cannot be found for low molecular weight polar mesogens and this is why they do not have a strong third order reflection either.

Looking at figure 6, ($P_8$ and $P_{12}$) we notice that the width of the central peak increases from 8 Å for $P_5$ to 13 Å for $P_{12}$. This may occur for two reasons:

Adding some aliphatic parts to the molecule decreases the mean value of the electron density and the overlap region then appears richer in electrons.

The overlap may increase with the size of the spacer and the overlaps given in table 2 and calculated on the basis of fully extended spacers may not be correct.

We must also remember that, polymer $P_{12}$ being crystalline at room temperature, figures 6(*c*) and 6(*d*) correspond to a temperature of 90°C and the central maximum may be spread out by thermal fluctuations compared to polymers $P_5$ and $P_8$.

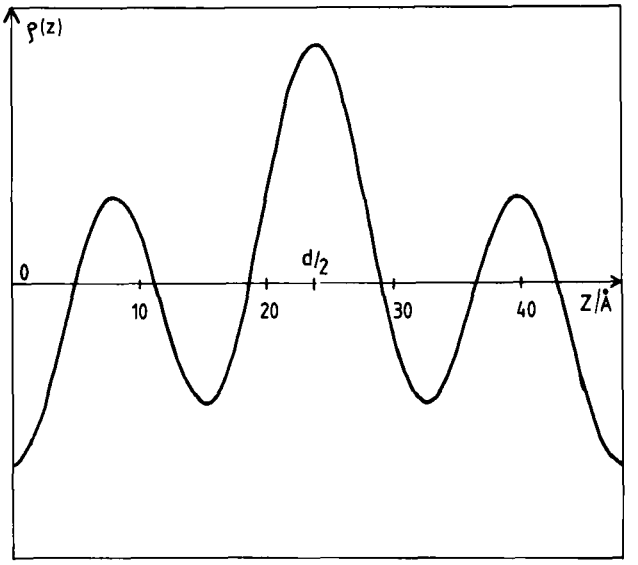


(*a*)

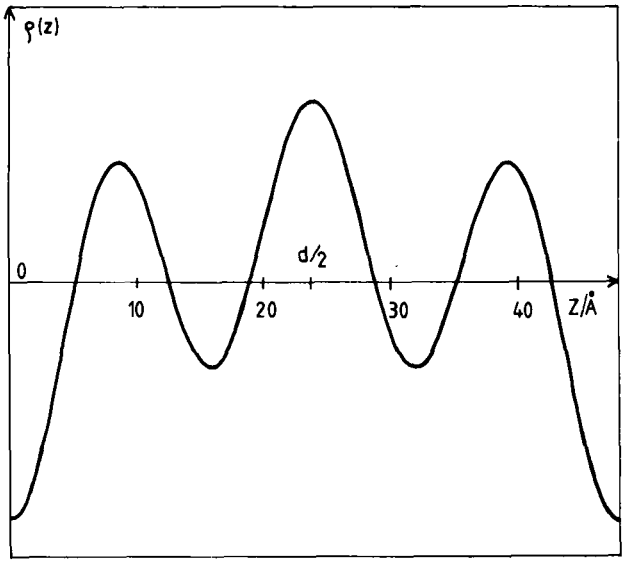


(*b*)

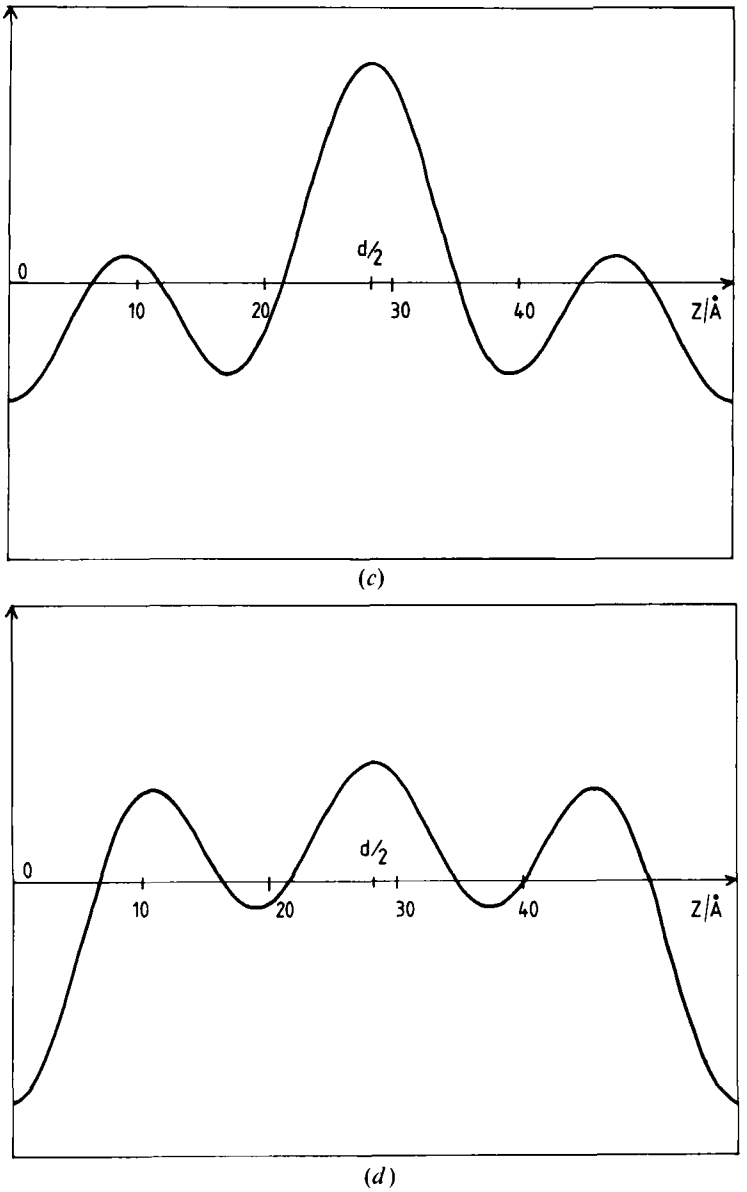


Figure 6. Possible electron density profiles for polymers $P_8$ and $P_{12}$; room temperature: (*a*) polymer $P_{8\varrho-+-}(z)$; (*b*) polymer $P_{8\varrho---}(z)$. $T = 90°C$: (*c*) polymer $P_{12\varrho-+-}(z)$; (*d*) polymer $P_{12\varrho---}(z)$.

## 4. Conclusion

All polymers $P_n$ are mesomorphic and possess a smectic $A_d$ phase as could be checked by optical microscopy, D.S.C. and X-ray diffraction. Oriented samples could be obtained either by use of a magnetic field or by drawing fibres. The molecular structure of the mesogenic cores induces a rather small overlap. When considering different polymers of the series, it is not quite clear whether the overlap should remain constant. Because of this small overlap and because the backbones tend to expand and squeeze the spacers, the electron density profile along the director $\varrho(z)$ is dominated by the contribution of the third order harmonic of period $d/3$. Varying the nature of

the backbone and that of the spacers may affect the intensity of this third order reflection. It might also be possible to predict theoretically the different widths along the director of the backbone, spacers and overlap by considering the elastic properties of these various parts of the system.

This work has been partly supported by a ATP-Mat-5-Polymères (CNRS) contract. We would like to thank Dr. P. Keller for the loan of microviscometer and we are also deeply indebted to Dr. A. M. Levelut and Dr. J. Doucet for helpful discussions and to Dr. A. Braslau for revising the English manuscript.

## Appendix

Preparation of 4-cyanobenzoylchloride **3** and 4-(4′-cyanobenzoyloxy)benzoylchloride **9**. These acid chlorides were prepared by the classical method using $SOCl_2$.

Preparation of benzyl 4-(4′-cyanobenzolyoxy)benzoate **7**. This compound was obtained by the reaction of **3** with **6** in pyridine at 70°C under a nitrogen atmosphere. Compound **7** was purified by crystallization from anhydrous ethanol. $T_F$ = 115°C yield: 62 g (86 per cent).

Preparation of 4-(4′-cyanobenzoyloxy)benzoic acid **8** 200 ml of trifluoroacetic acid and 30 ml of a solution of HBr in acetic acid (33 per cent, Merck) were added slowly to 53·55 g (0·15 mole) of compound **7** at room temperature and stirred for 4 hours. The reaction mixture was poured onto 500 g of crushed ice. The white precipitate was then filtered off, washed several times with water and acetone, and then dried. Compound **8** is mesomorphic: K254 S decomposition I. The yield was 32 g (80 per cent).

Preparation of the (ω-hydroxy-*n*-alkyl)4-(4′-cyanobenzoyloxy)benzoates **11**. The alkyl compounds **11** were obtained by reaction of **8** with an excess of the corresponding diol in pyridine under a nitrogen atmosphere. They were purified by silica column chromatography (eluent: chloroform). The yields and the fusion temperatures of compounds **11** are given in table 4:

Table 4. Yields and fusion temperatures $T_F$ of compounds **11**.

| *n* | % yield | $T_F$/°C |
|---|---|---|
| 4 | 36 | 80 |
| 5 | 65 | 84 |
| 6 | 43 | 79 |
| 7 | 53 | 92 |
| 8 | 32 | 80 |
| 9 | 53 | 75 |
| 10 | 43 | 85 |
| 12 | 46 | 99 |

Preparation of the 4-(4′-cyanobenzoyloxy)benzoyloxy ω-*n*-alkyl acrylates **14**. Compounds **14** were obtained in the classical way by reacting acrylic acid chloride with compounds **11** in N-dimethylaniline. They were purified in the same way as compounds **11**. The yields and the transition temperatures are shown in table 5.

Preparation of the poly[4-(4′-cyanobenzoyloxy)benzoyloxy ω-*n*-alkyl acrylate]s **1**. The polymerizations were carried out for 24 hours at 80°C in toluene and under a nitrogen atmosphere, using benzoyl peroxide as an initiator [concentration: 0·6 mol %].

Table 5. Yields and fusion temperatures $T_F$ of compounds **14**.

| $n$ | % yield | $T_F$/°C |
|---|---|---|
| 4 | 87 | 60 |
| 5 | 77 | 61 |
| 6 | 83 | 59 |
| 7 | 72 | 54 |
| 8 | 83 | 59 |
| 9 | 78 | 63 |
| 10 | 90 | 62 |
| 12 | 79 | 62 |

Polymers $P_n$ were purified twice by reprecipitation from chloroform solution into ether. The conversion yields were $n = 4$: 70 per cent; $n = 5$: 83 per cent; $n = 6$: 66 per cent; $n = 7$: 70 per cent; $n = 8$: 92 per cent; $n = 9$: 74 per cent; $n = 10$: 68 per cent; $n = 12$: 84 per cent.

## References

[1] FINKELMANN, H., RINGSDORF, H., and WENDORFF, J. R., 1978, *Makromolek. Chem.*, **179**, 273.

[2] FINKELMANN, H., and REHAGE, G., 1980, *Makromolek. Chem. rap. Commun.*, **1**, 31.

[3] See for instance GEMMEL, P. A., GRAY, G. W., and LACEY, D., 1985, *Molec. Crystals liq. Crystals*, **122**, 205. KOSTROMIN, S. G., TALROZE, R. V., SHIHAEV, V. P., and PLATE, N. A., 1982, *Makromolek. Chem. rap. Commun.*, **3**, 803. ZENTEL, R., and STROBL, G. R., 1984, *Makromolek. Chem.*, **185**, 2669. MAUZAC, M., HARDOUIN, F., RICHARD, H., ACHARD, M. F., SIGAUD, G., and GASPAROUX, H., 1986, *Eur. Polymer J.*, **22**, 137. LE BARNY, P., DUBOIS, J. C., FRIEDRICH, C., and NOEL, C., 1986, *Polymer Bull.*, **15**, 341.

[4] TINH, N. H., 1983, *J. Chim. phys.*, **80**, 83. See also the paper by HARDOUIN, F., LEVELUT, A. M., ACHARD, M. F., and SIGAUD, G., 1983, *J. Chim. phys.*, **80**, 53.

[5] LEVELUT, A. M., TARENTO, R. J., HARDOUIN, F., ACHARD, M. F., and SIGAUD, G., 1981, *Phys. Rev.* A, **24**, 2180.

[6] DAVIDSON, P., KELLER, P., and LEVELUT, A. M., 1985, *J. Phys., Paris*, **46**, 939.

[7] See for instance RICHARDSON, R. M., and HERRING, N. J., 1985, *Molec. Crystals liq. Crystals*, **123**, 143. SUTHERLAND, H. H., BASU, S., and RAWAS, A., 1987, *Molec. Crystals liq. Crystals*, **145**, 73.

[8] DE GENNES, P. G., 1974, *The Physics of Liquid Crystals* (Clarendon Press).

[9] GUDKOV, V. A., 1984, *Sov. Phys. Crystallogr.*, **29**, 316.